Mech Time-Depend Mater (2012) 16:1–18
DOI 10.1007/s11043-011-9132-2

Theoretical and computational modelling of instrumented indentation of viscoelastic composites

Yan-Ping Cao · Ke-Lin Chen

Received: 22 April 2010 / Accepted: 4 January 2011 / Published online: 15 January 2011

Abstract In this study, we investigate the indentation of viscoelastic composites. The composite is assumed to consist of two phases, i.e., the filler and the matrix, which are linear elastic and linear viscoelastic material, respectively. Two cases are investigated: (1) hard fillers are scattered in a very soft matrix; (2) the matrix is much harder than the fillers. Particular attention is paid to the correlation between the indentation relaxation loads and the material and geometric parameters of the composite system. To this end, we perform a theoretical analysis which is followed by finite element analysis. Our main result is a simple relation correlating the reduced relaxation modulus of the matrix, $E_{m,r}(t)$, with the indentation relaxation load $P(t)$, i.e., $E_{m,r}(t) = P(t)/P(0)$, where $P(0)$ represents the indentation load at the starting point of the relaxation test. This result on one hand indicates that for the two cases under study the relaxation feature of the indentation load is determined by the reduced relaxation modulus of the matrix. On the other hand, the result shows that the reduced relaxation modulus of the matrix of the composites may be simply determined from the indentation relaxation load without invoking the knowledge of both the indenter geometry and the profile of indented solids.

Keywords Indentation · Viscoelastic composites · Finite element simulation

1 Introduction

Many natural biological materials, ranging from the articular cartilage, vasculars to cells, are viscoelastic composites from the viewpoint of material science. Determining the mechanical properties of these viscoelastic biological materials is of great importance for the tissue engineering as well as for understanding the responses of cells or tissues to the mechanical stimuli (Levental et al. 2007; Lee et al. 2010). In addition, man-made biocomposites have received much attention during the past decades, which may be formed

Y.-P. Cao (✉) · K.-L. Chen
Applied Mechanics Lab, Department of Engineering Mechanics, Tsinghua University, Beijing 100084, China
e-mail: caoyanping@tsinghua.edu.cn

by a matrix and the fillers (e.g. particles or fibers). Biocomposites find wide applications such as in drug delivery, tissue engineering and cosmetic industry (Thomas et al. 2007; Ramakrishna et al. 2004). Mechanical characterization of the composites as well as each constituent in many cases is crucial not only for their practical use, but also for understanding the connection between the microstructures and properties of the materials, and further optimizing the processing procedures. Instrumented indentation, which has been proved to be a powerful tool for mechanical characterization of time-dependent materials (e.g. Shimizu et al. 1999; Fischer-Cripps 2004; Lu et al. 2003; Cheng and Cheng 2004; Cheng et al. 2006; Ngan et al. 2005; Ebenstein and Pruitt 2006; Huang and Lu 2006; Cheng and Yang 2009; Oyen and Cook 2003; Oyen 2007; Herbert et al. 2009; Cao 2007; Cao et al. 2009) in recent years, appears to be an efficient tool for evaluating the mechanical properties of viscoelastic composite materials, especially at a local area and/or at small scales.

In this study, we investigate the indentation of a typical composite system consisting of two constituents, i.e., the matrix and the filler, which are linear viscoelastic and linear elastic, respectively. The objective is to reveal the correlation between the relaxation feature of the indentation loads and geometric and material parameters of the composite system. To this end, a combination of theoretical and computational analysis has been carried out. The results together with the conclusions made in this study may improve the current understanding of the indentation of viscoelastic composite materials.

2 Theoretical analysis

Figure 1 illustrates the indentation of a two-phase composite system using a rigid indenter. In this study, it is assumed that the matrix and the fillers are perfectly bonded. Effects of the interface phase are omitted although they may play important roles in many cases.

We first consider the indentation of a rigid indenter with arbitrary profile indenting into a composite with arbitrary shape (Fig. 1), for which both phases are homogeneous, isotropic

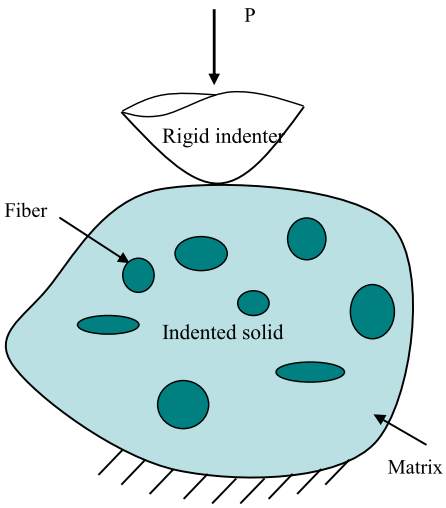

Fig. 1 Schematic drawing of a rigid indenter indenting into a composite solid

and linear elastic materials and the constitutive relations read

$$\sigma_{ij,(m)} = 2G_m\varepsilon_{ij,(m)} + \lambda_m\delta_{ij}\varepsilon_{kk,(m)} = \frac{E_m}{1+v_m}\varepsilon_{ij,(m)} + \frac{E_m v_m}{(1+v_m)(1-2v_m)}\delta_{ij}\varepsilon_{kk,(m)}, \quad (1a)$$

$$\sigma_{ij,(f)} = 2G_f\varepsilon_{ij,(f)} + \lambda_f\delta_{ij}\varepsilon_{kk,(f)} = \frac{E_f}{1+v_f}\varepsilon_{ij,(f)} + \frac{E_f v_f}{(1+v_f)(1-2v_f)}\delta_{ij}\varepsilon_{kk,(f)}, \quad (1b)$$

where σ_{ij} $(i = 1, 2, 3;\ j = 1, 2, 3)$ and ε_{ij} are the components of the stress and strain tensors, respectively, ε_{kk} $(k = 1, 2, 3)$ is the dilatational strain, λ is Lamé constant and G the shear modulus. E is Young's modulus, and v is Poisson's ratio. δ_{ij} represents Kronecker delta. The subscripts 'm' and 'f' represent the matrix and the filler and are not numbers, respectively. Under given boundary conditions, the indentation load P may be a function of the following independent parameters:

$$P = g(h, E_m, E_f, v_m, v_f, c_0, c_1, c_2, \ldots, c_M, d_0, d_1, d_2, \ldots, d_N, e_0, e_1, e_2, \ldots, e_K), \quad (2)$$

where h is indenter displacement. $c_0, c_1, c_2, \ldots, c_M$ (M is a finite integer) are the geometric parameters used to describe the profile of the indenter in the contact region, and $d_0, d_1, d_2, \ldots, d_N$ (N is a finite integer) are the parameters describing the shape of the indented solid that affect the indentation responses. $e_0, e_1, e_2, \ldots, e_K$ (K is a finite integer) are the parameters representing the positions and geometric shapes of the fillers. The geometric parameters c_ξ $(0 \le \xi \le M)$, d_η $(0 \le \eta \le N)$ and e_ς $(0 \le \varsigma \le K)$ should have the following dimensions

$$[c_\xi] = [h]^{R_\xi}, \quad (3a)$$

$$[d_\eta] = [h]^{r_\eta}, \quad (3b)$$

$$[e_\varsigma] = [h]^{b_\varsigma}, \quad (3c)$$

where R_ξ, r_η and b_ς are real numbers. Among the governing parameters in (2), the indenter displacement h and the modulus of the matrix E_m have the independent dimensions. Applying Pi-theorem in dimensional analysis (Barenblatt 1996) to (2) leads to

$$P = E_m h^2 \Pi\left(\begin{matrix} v_f, v_m, \frac{c_0}{h^{R_0}}, \frac{c_1}{h^{R_1}}, \frac{c_2}{h^{R_2}}, \ldots, \frac{c_M}{h^{R_M}}, \frac{d_0}{h^{r_0}}, \frac{d_1}{h^{r_1}}, \frac{d_2}{h^{r_2}}, \ldots, \frac{d_N}{h^{r_N}}, \\ \frac{e_0}{h^{b_0}}, \frac{e_1}{h^{b_1}}, \frac{e_2}{h^{b_2}}, \ldots, \frac{e_K}{h^{b_K}}, \frac{E_f}{E_m} \end{matrix}\right), \quad (4)$$

where Π is a dimensionless function.

In this study, we are interested in two cases: (1) hard fillers are embedded in a very soft matrix; and (2) the matrix is much harder than the fillers. For both cases, it is assumed that the dimensionless parameter E_m/E_f may drop out of (4), the physics behind this assumption will be addressed in detail below, and the indentation load-depth relation may be given by

$$P = E_m h^2 \Pi\left(\begin{matrix} v_f, v_m, \frac{c_0}{h^{R_0}}, \frac{c_1}{h^{R_1}}, \frac{c_2}{h^{R_2}}, \ldots, \frac{c_M}{h^{R_M}}, \frac{d_0}{h^{r_0}}, \frac{d_1}{h^{r_1}}, \frac{d_2}{h^{r_2}}, \ldots, \frac{d_N}{h^{r_N}}, \\ \frac{e_0}{h^{b_0}}, \frac{e_1}{h^{b_1}}, \frac{e_2}{h^{b_2}}, \ldots, \frac{e_K}{h^{b_K}} \end{matrix}\right) = E_m \Psi(h), \quad (5)$$

where

$$\Psi(h) = h^2 \Pi\left(\begin{matrix} v_f, v_m, \frac{c_0}{h^{R_0}}, \frac{c_1}{h^{R_1}}, \frac{c_2}{h^{R_2}}, \ldots, \frac{c_M}{h^{R_M}}, \frac{d_0}{h^{r_0}}, \frac{d_1}{h^{r_1}}, \frac{d_2}{h^{r_2}}, \ldots, \frac{d_N}{h^{r_N}}, \\ \frac{e_0}{h^{b_0}}, \frac{e_1}{h^{b_1}}, \frac{e_2}{h^{b_2}}, \ldots, \frac{e_K}{h^{b_K}} \end{matrix}\right). \quad (6)$$

We further investigate the above indentation problem by assuming that the matrix material is linear viscoelastic instead of linear elastic, and the stress-strain relation given by

$$\sigma_{ij,(m)}(t) = \int_0^t \left[2G_m(t-\tau)\frac{\partial \varepsilon_{ij,(m)}(\tau)}{\partial \tau} + \lambda_m(t-\tau)\delta_{ij}\frac{\partial \varepsilon_{kk,(m)}(\tau)}{\partial \tau} \right] \mathrm{d}\tau, \tag{7}$$

G_m and λ_m in the time domain are related to the relaxation modulus $E_m(t)$ and Poisson's ratio $v_m(t)$ by

$$G_m(t) = \frac{E_m(t)}{2(1+v_m(t))}, \tag{8}$$

$$\lambda_m(t) = \frac{E_m(t)v_m(t)}{(1+v_m(t))(1-2v_m(t))}. \tag{9}$$

Assuming a time-independent Poisson's ratio, invoking the elastic-viscoelastic correspondence principle (Christensen 1982), the indentation load-depth relation obtained from (5) by replacing the elastic modulus E_m with $\bar{E}_m(s)s$ can be given by

$$\bar{P}(s) = \bar{E}_m(s)s\Psi(\bar{h}(s)) \tag{10}$$

where $\bar{E}_m(s)$ is the Laplace transform of the relaxation modulus $E_m(t)$, s is the transform variable. $\bar{P}(s)$ and $\bar{h}(s)$ represent the Laplace transform of the indentation load $P(t)$ and the indenter displacement $h(t)$, respectively. The inverse Laplace transform of (10) gives

$$P(t) = \int_0^t E_m(t-\tau)\mathrm{d}\Psi. \tag{11}$$

The traditional elastic-viscoelastic correspondence principle is limited to the case where boundary conditions are time-independent, although the extended correspondence principle may attack the problems with moving boundaries (Christensen 1982). This study focuses on the indentation relaxation test in which the indenter displacement is kept as constant. Our finite element analysis shows that contact area in this case basically does not change and thus, indeed, the elastic-viscoelastic correspondence principle may be reliably adopted. For a spherical, conical or Berkovich indenter indenting into a homogeneous half-space, (11) degenerates to the results reported in the literature (Graham 1965; Giannakopoulos 2006).

Equation (11) may be further written as

$$P(t) = \int_0^t E(t-\tau)\frac{\mathrm{d}\Psi}{\mathrm{d}h}\frac{\mathrm{d}h}{\mathrm{d}\tau}\mathrm{d}\tau. \tag{12}$$

As aforementioned, we consider a relaxation test, in which the indenter displacement is described via a Heaviside step function,

$$h = \begin{cases} h_0 & (t \geq 0), \\ 0 & (t < 0). \end{cases} \tag{13}$$

Inserting (13) into (12) reads

$$P(t) = \int_0^t E_m(t-\tau)\frac{\mathrm{d}\Psi}{\mathrm{d}h}h_0\delta(\tau)\mathrm{d}\tau, \tag{14}$$

where δ is the Dirac delta function. According to the integral property of the Dirac delta function, (14) becomes

$$P(t) = E_m(t) h_0 \left. \frac{\mathrm{d}\Psi}{\mathrm{d}h} \right|_{h=h_0}. \tag{15}$$

It is noted that the parameter $h_0(\mathrm{d}\Psi/\mathrm{d}h)|_{h=h_0}$ in (15) is independent of time for a time-independent Poisson's ratio. The relaxation modulus of the matrix may be written in the following form (Fung 1993)

$$E_m(t) = E_{m,0} E_{m,r}(t), \tag{16}$$

where $E_{m,0}$ is the instantaneous modulus, representing the stiffness of a viscoelastic material at the instantaneous time when the external load acts, and $E_{m,r}(t)$ is the reduced relaxation modulus (normalized relaxation modulus) which indicates the relaxation property of a viscoelastic material.

Inserting (16) into (15) leads to

$$E_{m,r}(t) = \frac{P(t)}{P(0)}, \tag{17}$$

where $P(0)$ is the indentation load at the starting point of relaxation. Equation (17) and the analysis above contain the following interesting and insightful information.

(i) The results indicate that when a direct problem is considered, the indentation loads depend on the material properties of both the matrix and the fillers, the geometric parameters of the system as well as the indentation depth. However, the relaxation feature of the contact loads may only depend on the reduced relaxation modulus of the matrix material and is independent of other geometric and material parameters.

(ii) From the viewpoint of inverse analysis, (17) shows that the reduced relaxation modulus of the matrix material can be measured simply from the indentation relaxation loads. It is not necessary to invoke the knowledge of the geometric parameters of the system (including the profiles of the indenter and the indented solids as well as the positions and shapes of the fillers) and the material properties of the fillers.

It should be noted that the derivation of (5) from (4) contains a key assumption, i.e., the dimensionless function Π in (4) is independent of E_m/E_f when E_m/E_f is sufficiently large or sufficiently small. Here, we provide an explanation on the physics behind this assumption. (1) When E_m/E_f is sufficiently large, i.e., the fillers are very soft compared to the matrix, the contribution of the fillers to the total strain energy of the system can be negligible and in this sense the fillers resemble the voids. (2) In the case that E_m/E_f is sufficiently small, indentation induced deformation is mainly accommodated by the matrix and the role played by fillers resembles that of rigid inclusions (Liu et al. 2005). Effects of both the voids and rigid inclusions on the indentation responses can be represented by the geometric parameters and the parameter E_m/E_f may be dropped out from (4). For the indentation of porous substrates ($E_f = 0$), which represents a limit of the case of $E_{m,l} \gg E_f$ as investigated in this paper, we have demonstrated the applicability of (17) (Cao et al. 2010). Here, $E_{m,l}$ is the long-term modulus of the matrix material. In next section, we will examine our theoretical result and the explanation above using finite element analysis.

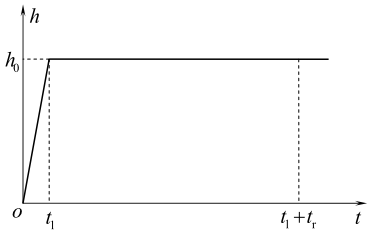

Fig. 2 Indentation displacement history used in the simulation of the indentation relaxation tests

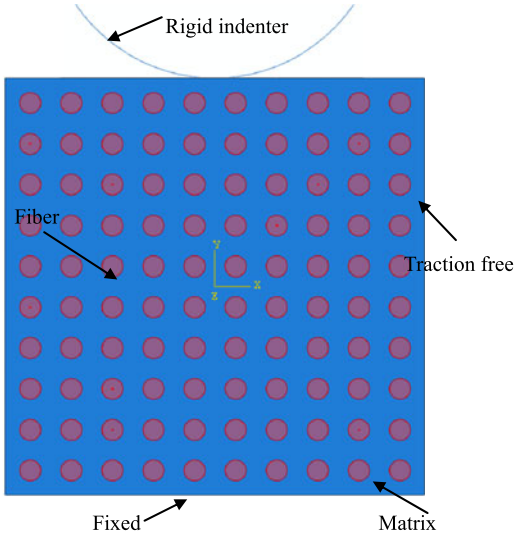

(a)

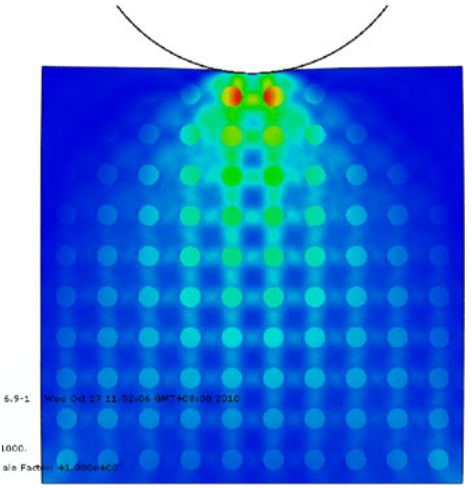

(b)

Fig. 3 Indentation of a cylindrical indenter into a composite substrate with uniform distribution of fibres. (**a**) Computational model; (**b**) Deformation of the substrate corresponding to the maximum indentation depth

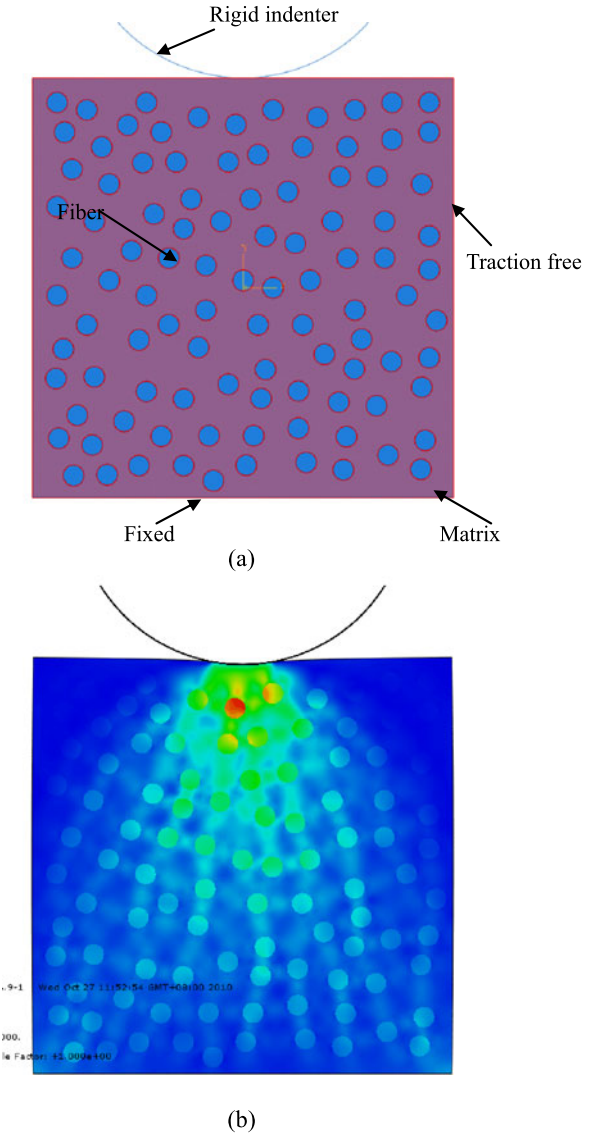

Fig. 4 Indentation of a cylindrical indenter into a composite substrate with random distribution of the fibres. (**a**) Computational model; (**b**) Deformation of the indented solid at the maximum indentation depth

3 Finite element analysis

Finite element analysis is performed using the commercial software ABAQUS (2008). Detail information involved in the simulations is given as follows.

3.1 Details of the computational modelling

In the simulations, the matrix material of the composite is assumed to be linear viscoelastic for which the relaxation modulus and Poisson's ratio are taken as $E_m(t) = 900[1 - 0.4(1 - e^{-t/100s})]$ MPa and $\upsilon_m = 0.4$, respectively (the material properties taken here are used for

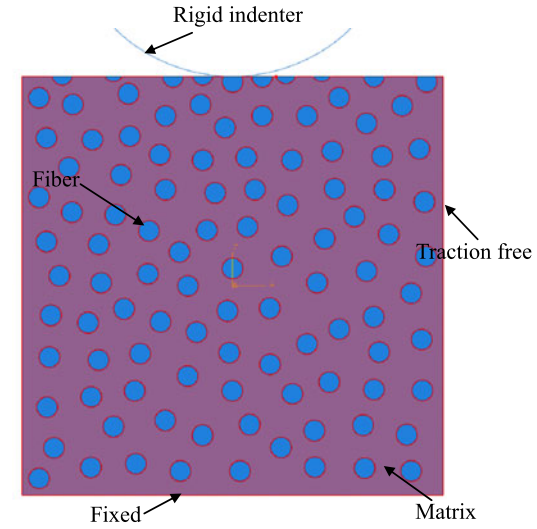

(a)

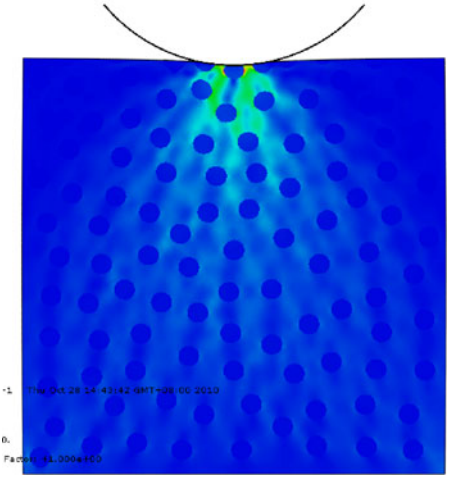

(b)

Fig. 5 Indentation of a cylindrical indenter into a composite substrate in which the fibres directly contact with the indenter. (**a**) Computational model; (**b**) Deformation of the indented solid at the maximum indentation depth

illustration, but the conclusions may apply to realistic systems). In this case, the matrix material has an instantaneous modulus $E_{m,0} = 900$ MPa, long-term modulus $E_{m,l} = 540$ MPa and the characteristic relaxation time of $t_c = 100$ s. The modulus of the fillers varies from 540 Pa to 100 GPa and v_f is taken as 0.3. The loading protocol adopted in the simulations is shown in Fig. 2, which is an approximation of the step function as given by (13). A good approximation requires that t_l at which the indentation displacement reaches its maximum value should be much smaller than t_c. Here we take $t_l = 0.05t_c = 5$ s. The relaxation time t_r is taken as 1000 s, which is much larger than the characteristic relaxation time of the material.

The following representative examples of practical interest are investigated.

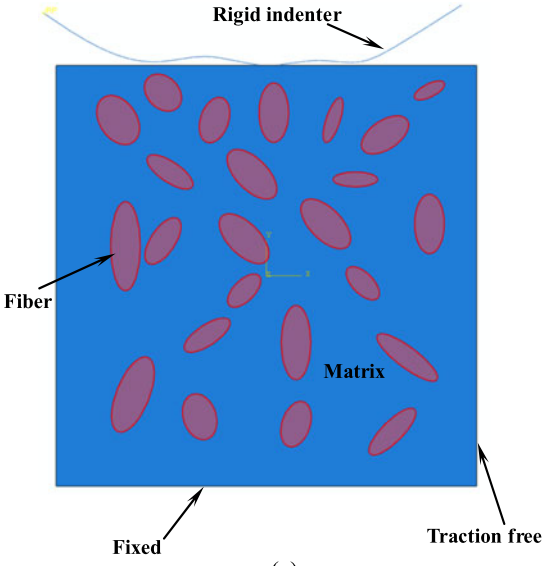

(a)

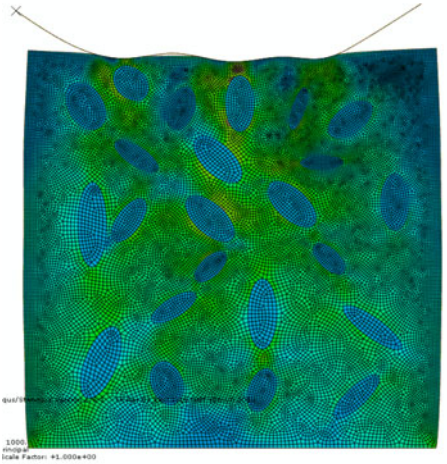

(b)

Fig. 6 A cylindrical indenter with irregular profile indenting into a linear viscoelastic substrate containing elastic fibres. (**a**) Computational model; (**b**) Deformation at the maximum indentation depth

(1) *Indentation of a cylindrical indenter into a composite substrate with uniform distribution of fibres*

In this example, a cylindrical indenter is assumed to indent into a linear viscoelastic substrate containing elastic fibres. Figure 3(a) gives our two-dimensional computational model. The bottom of the indented solid is fixed with other boundaries traction free. The fibres are uniformly distributed in the matrix. A total of 36264 four-node bilinear plane strain quadrilateral elements with reduced integration and hourglass control (CPE4R) are used to model the fibres and the matrix. The deformed indented solid is shown as Fig. 3(b).

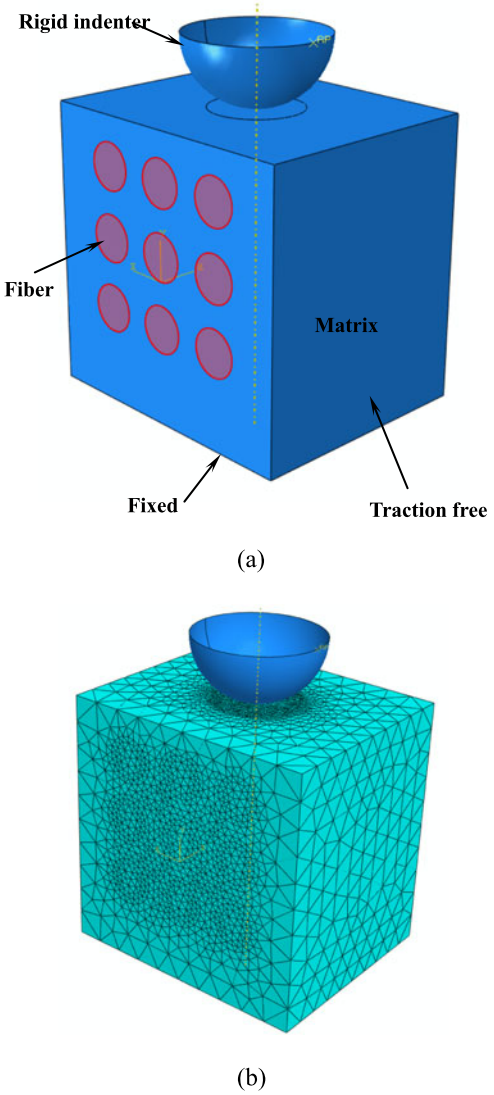

Fig. 7 A spherical indenter indenting into a fibre reinforced composite substrate. (**a**) Computational model; (**b**) Finite element mesh

(2) *Indentation of a cylindrical indenter into a composite substrate with random distribution of the fibres*

This example represents a cylindrical indenter indenting into a linear viscoelastic substrate containing non-uniform distribution of elastic fibres. The volume ratio of the fibres in this example is the same as that in Example (1). Figure 4(a) gives the computational model together with the boundary conditions. The finite element model contains 30544 CPE4R elements. The bottom of the indented solid is fixed with other boundaries traction free. Figure 4(b) represents the deformation of the indented solid at the maximum indentation depth.

(3) *Indentation of a cylindrical indenter into a composite substrate in which the fibres directly contact with the indenter*

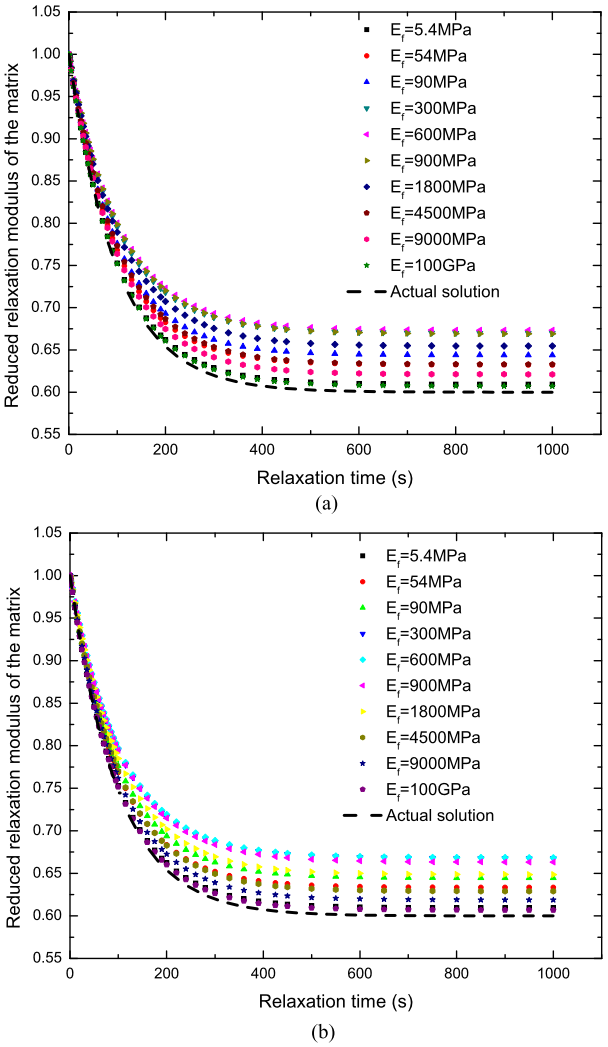

Fig. 8 A comparison of the identified matrix reduced relaxation modulus $E_{m,r}(t)$ with actual solutions. (**a**) Example (1); (**b**) Example (2); (**c**) Example (3); (**d**) Example (4)

In the previous two examples, the elastic fibres are embedded in the matrix. Here we investigate the case in which the fibres may directly contact with the indenter. Figure 5(a) shows our two-dimensional computational model consisting of 36816 four-node bilinear plane strain quadrilateral elements with reduced integration and hourglass control. The boundary conditions are the same as those given in Examples (1) and (2). The deformed indented solid is shown as Fig. 5(b).

(4) *Indentation of a indenter with irregular shape into a composite substrate*

In the Examples (1), (2) and (3), the fibres with circular cross-section and the indenter with regular profile are investigated. In this example, we study the case in which a indenter with irregular profile is assumed to indent into a linear viscoelastic substrate containing

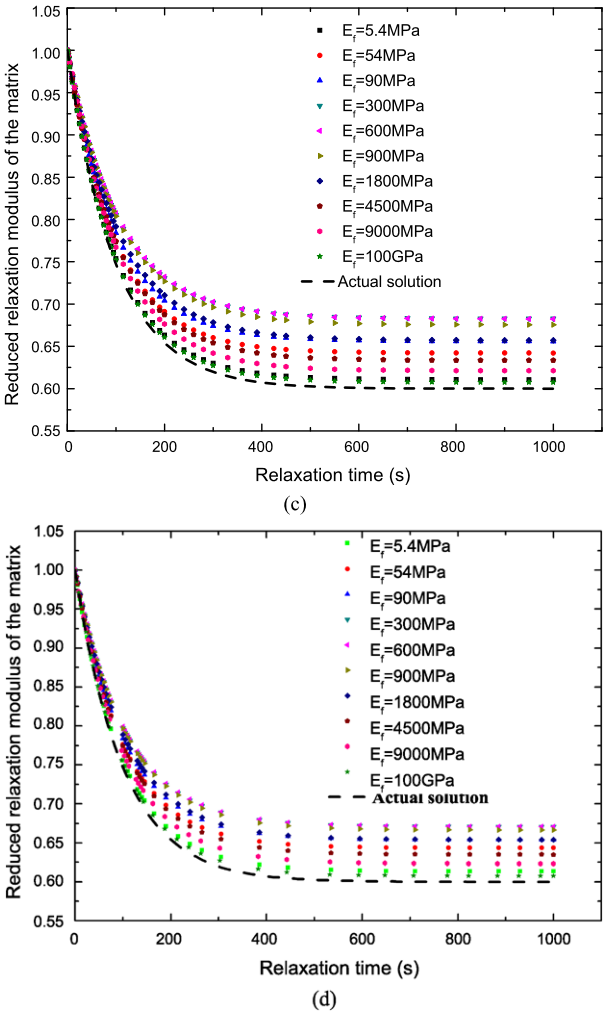

Fig. 8 (*Continued*)

elastic fibres with elliptical cross-section. Figure 6(a) illustrates the computational model containing 27165 CPE4R elements. The bottom of the indented solid is fixed with other boundaries traction free. Figure 6(b) shows the deformed indented solid.

(5) *A spherical indenter indenting into a fibre reinforced composite substrate*

The examples above represent two dimensional indentation problems. A three-dimensional example is further considered. We investigate a spherical indenter indenting into a fibre-reinforced composite. Figure 7 illustrates the computational model which contains a total of 160 371 linear tetrahedral elements (C3D4). Very fine mesh is used in the contact region in order to guarantee the convergence of the computational results. The boundary conditions used in the analysis are given in Fig. 7(a).

In all the examples above, the mesh qualities are checked to avoid extreme distortions and the convergences are ensured. The relaxation loads-time relations are recorded, which

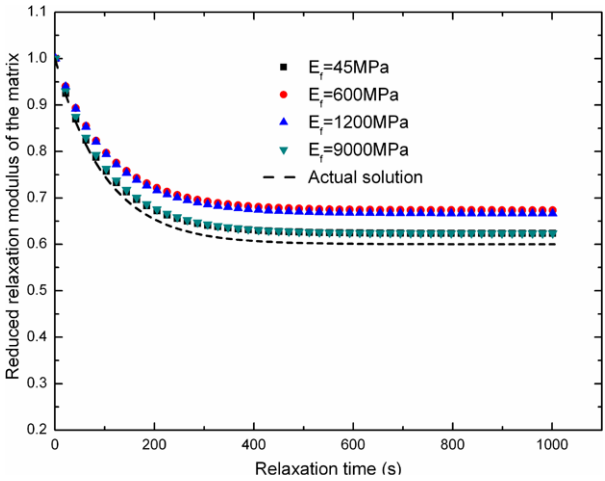

Fig. 9 A comparison of the identified matrix reduced relaxation modulus $E_{m,r}(t)$ with actual solution for Example (5)

will be used together with (17) to determine the reduced relaxation modulus of the matrix as discussed in detail below.

3.2 Results and discussions

For the examples above, we focus on the displacement-controlled indentation. The reduced relaxation moduli of the matrix materials are determined from the computed relaxation load-time relation and (17). Figure 8 shows a comparison of the identified results with the actual solutions for Examples (1)∼(4). Figure 9 represents the comparison of the identified matrix reduced relaxation modulus based on (17) to the actual solution for Example (5). The results in these figures show that when $E_{m,l}/E_f$ or $E_f/E_{m,0}$ is sufficiently large, e.g. larger than 10, (17) as given by the theoretical analysis works well for all the examples.

In our theoretical analysis, the elastic-viscoelastic correspondence principle is adopted assuming that the contact area does not change during the indentation relaxation test. We carefully examine this assumption by examining the variation in the contact area throughout the indentation relaxation procedure. We find that for all the examples under study, indeed, the contact areas basically do not change as illustrated in Fig. 10. The figure shows the deformation of the indented solid near to the indenter corresponding to different relaxation time for Example (4).

The representative examples presented above demonstrate the validity of our theoretical analysis to the indentation problems of practical interest. Nevertheless, the limitations in the theoretical analysis should be emphasized.

First, the constitutive law of the matrix involved in this study is limited to the linear viscoelastic model. For the indentation of nonlinear viscoelastic materials, the theoretical analysis and conclusions drawn herein may be invalid. In addition, the present study is limited to the case where the Poisson's ratio is time-independent and the instantaneous modulus and characteristic relaxation time do not change with loading. It is noted that these assumptions have been adopted in quite a few previous publications (e.g. Shimizu et al. 1999; Cheng et al. 2006; Oyen 2005) and are indeed reasonable for various viscoelastic materials in engineering.

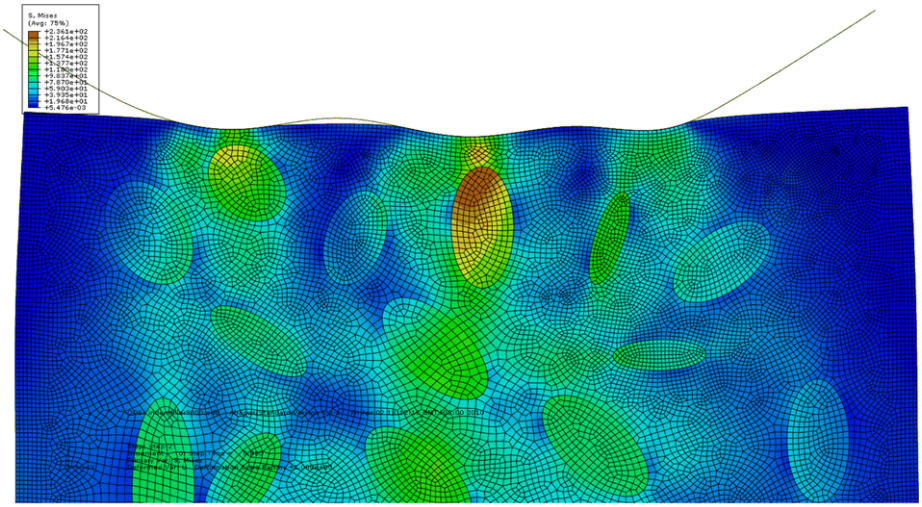

(a)

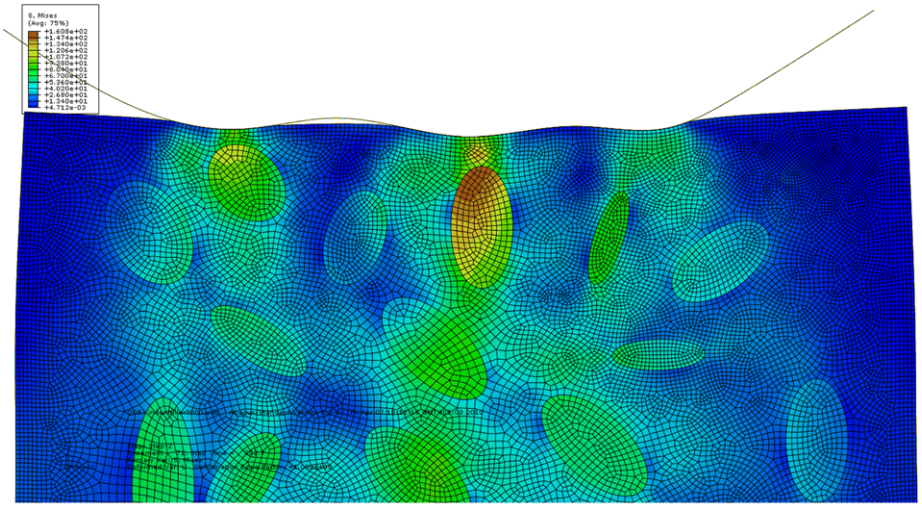

(b)

Fig. 10 Variation of the contact area with the indentation relaxation time for Example (4) and the case of $E_f = 9000$ MPa. (**a**) $t = 0$ s; (**b**) $t = 302$ s; (**c**) $t = 602$ s; (**d**) $t = 1000$ s

Second, it is pointed out that in this study we focus on the circumstances where the fillers are much softer or harder than the matrix so that their effects on the indentation responses can be represented by the geometric parameters. It is important to mention a very critical situation, i.e., indentation is performed on single fibre or particle. In this case, determining the relaxation property of the matrix from the indentation responses and (17) appears to be unreliable especially when the deformation is mainly confined at a local area of the fibre/particle. In order to illustrate this point, we investigate an axisymmetric rigid cone indenting into a particle surrounded by the matrix, Fig. 11(a). Figure 11(b) gives the deformation of the indented solid at the maximum indentation depth. The relax-

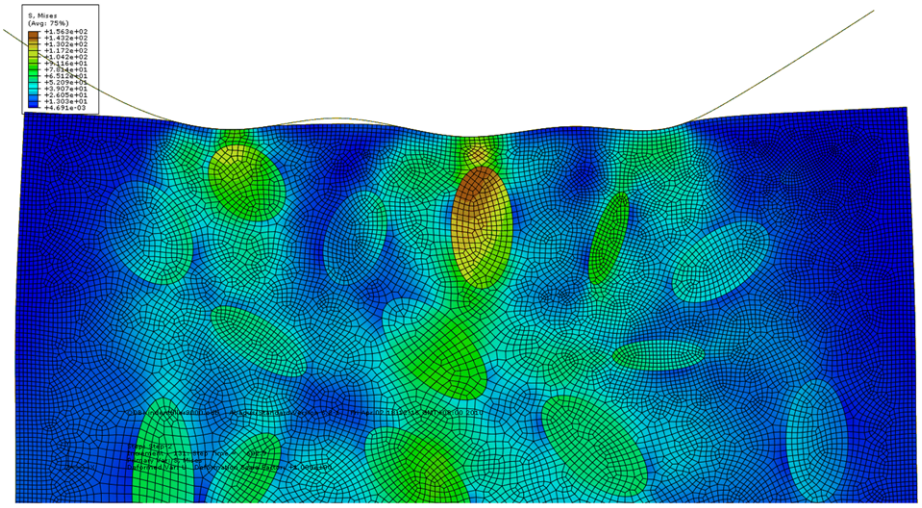

(c)

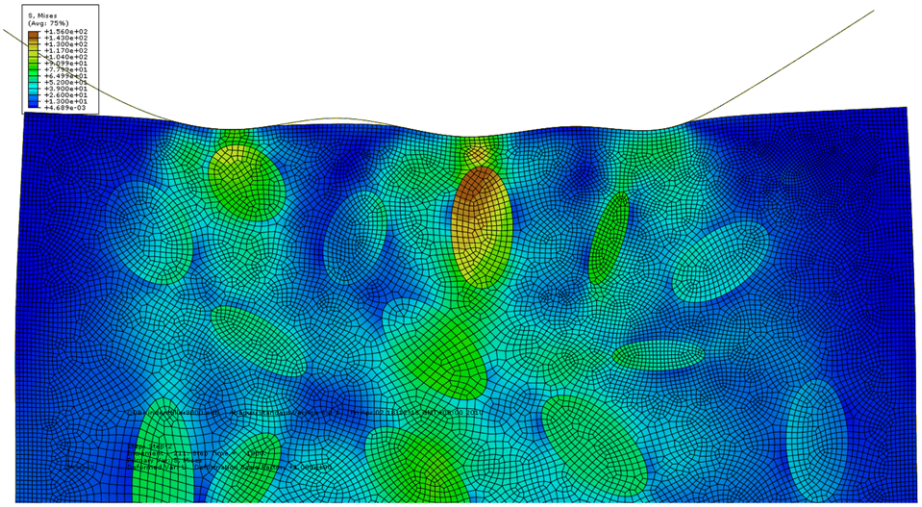

(d)

Fig. 10 (*Continued*)

ation loads together with (17) are adopted to determine the reduced relaxation modulus of the matrix and the results given in Fig. 12. It is seen that the identified results are far from the actual solution. This is because that in this case the particle makes major contribution to the strain energy of the system although the particle is much softer than the matrix as shown in Fig. 11(b). Thus assumption made in the derivation of (5) from (4) is invalid.

Finally, it is emphasized that the theoretical analysis performed here is restricted to the two phase composite system. When the interface phase plays a key role in a system, caution should be taken when using the results as well as the conclusions achieved in this study.

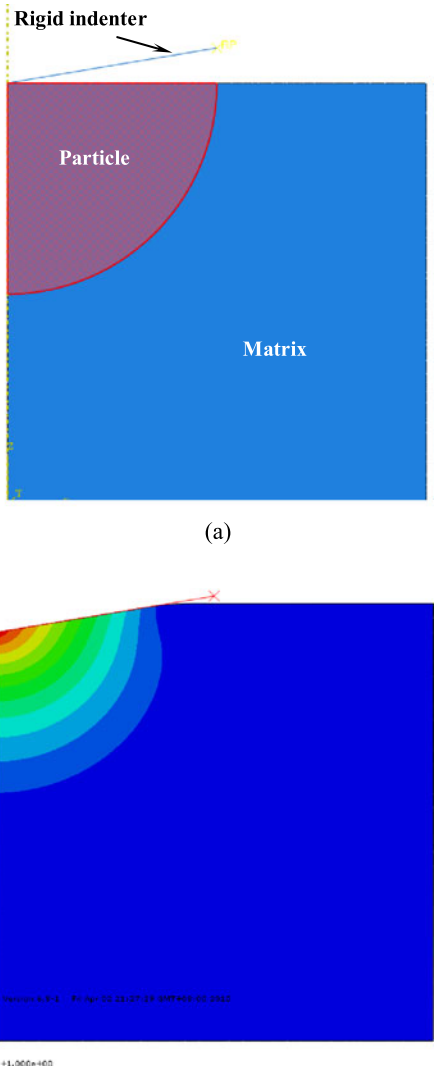

Fig. 11 A conical indenter indenting into a single particle embedded in a linear viscoelastic matrix. (**a**) Computational model; (**b**) Deformation of the indented solid for the case of $E_f = 54$ MPa

4 Conclusions

In this study, we address the indentation of a two-phase composite system in which the matrix material is a linear viscoelastic and the fillers are a linear elastic material. In summary, the following contributions have been made.

Our theoretical analysis performed on a rigid indenter with arbitrary profile indenting into a composite with arbitrary shape reveals a simple correlation between the indentation relaxation loads and the reduced relaxation modulus of the matrix $E_{m,r}(t)$. On one hand, the relation indicates that the relaxation feature of the contact loads is determined by $E_{m,r}(t)$ and basically independent of other geometric and material parameters of the system provided that the fillers are much harder or softer than the matrix. On the other hand, our

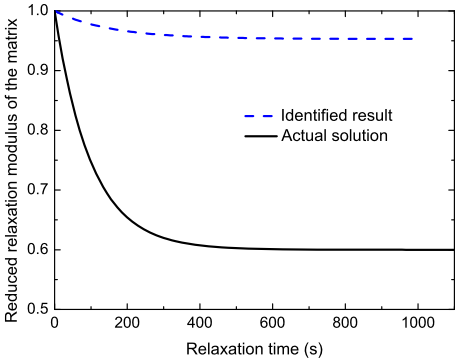

Fig. 12 A comparison of the identified reduced relaxation modulus of the matrix to the real solution (the indent is on the filler, $E_f = 54$ MPa)

analysis shows that $E_{m,r}(t)$ may be measured using indentation relaxation loads and the simple relation reported here. Numerical experiments based on finite element analysis have been carried out to identify the extent to which the theoretical result is effective. The results reported in this study together with the discussions provide insightful information and may help understand instrumented indentation of viscoelastic composites, which may include some biological soft tissues and man-made biocomposites.

Acknowledgements Supports from the National Natural Science Foundation of China (Grant No. 10972112) and 973 Program (No. 2010CB631005) are acknowledged. Statement: This is a special issue paper, the main results have been presented in SEM 2010 annual meeting and included in the conference paper.

References

ABAQUS User's Manual, version 6.8: Providence: Hibbit, Karlsson & Sorenson (2008)
Barenblatt, G.I.: Scaling, Self-similarity and Intermediate Asymptotics. Cambridge University Press, Cambridge (1996)
Cao, Y.P.: Determination of the creep exponent of a power-law creep solid using indentation tests. Mech. Time-Depend. Mater. **11**, 159–172 (2007)
Cao, Y.P., Ma, D.C., Raabe, D.: The use of flat punch indentation to determine the viscoelastic properties in the time and frequency domains of a soft layer bonded to a rigid substrate. Acta Biomaterialia **5**, 240–248 (2009)
Cao, Y.P., Ji, X.Y., Feng, X.Q.: Geometry independence of the normalized relaxation functions of viscoelastic materials in indentation. Philos. Mag. **90**, 1639–1655 (2010)
Cheng, Y.T., Cheng, C. M.: Scaling, dimensional analysis, and indentation measurements. Mater. Sci. Eng., R Rep. **44**, 91–149 (2004)
Cheng, Y.T., Yang, F.Q.: Obtaining shear relaxation modulus and creep compliance of linear viscoelastic materials from instrumented indentation using axisymmetric indenters of power-law profiles. J. Mater. Res. **24**, 3013–3017 (2009)
Cheng, Y.T., Ni, W.Y., Cheng, C.M.: Nonlinear analysis of oscillatory indentation in elastic and viscoelastic solids. Phys. Rev. Lett. **97**, 075506 (2006)
Christensen, R.M.: Theory of Viscoelasticity: An Introduction. Academic Press, San Diego (1982)
Ebenstein, D.M., Pruitt, L.A.: Nanoindentation of biological materials. Nano Today **1**, 26 (2006)
Fischer-Cripps, A.C.: Multiple-frequency dynamic nanoindentation testing. J. Mater. Res. **19**, 2981–2989 (2004)
Fung, Y.C.: Biomechanics: Mechanical Properties of Living Tissues. Springer, New York (1993)
Giannakopoulos, A.E.: Elastic and viscoelastic indentation of flat surfaces by pyramid indentors. J. Mech. Phys. Solids **54**, 1305–1332 (2006)
Graham, G.A.C.: The contact problem in the linear theory of viscoelasticity. Int. J. Eng. Sci. **3**, 27–45 (1965)
Herbert, E.G., Oliver, W.C., Lumsdaine, A., Pharr, G.M.: Measuring the constitutive behavior of viscoelastic solids in the time and frequency domain using flat punch nanoindentation. J. Mater. Res. **24**, 626–637 (2009)

Huang, G., Lu, H.B.: Measurement of Young's relaxation modulus using nanoindentation. Mech. Time-Depend. Mater. **10**, 229–243 (2006)

Levental, I., Georges, P.C., Janmey, P.A.: Soft biological materials and their impact on cell function. Soft Matter **3**, 299–206 (2007)

Lee, B., Han, L., Frank, E.H., Chubinskaya, S., Ortiz, C., Grodzinsky, A.J.: Dynamic mechanical properties of the tissue-engineered matrix associated with individual chondrocytes. J. Biomech. **43**, 469–476 (2010)

Liu, Y.J., Nishimura, N., Otani, Y.: Large-scale modeling of carbon-nanotube composites by a fast multipole boundary element method. Comput. Mater. Sci. **34**, 173–187 (2005)

Lu, H., Wang, B., Ma, J., Huang, G., Viswanathan, H.: Measurement of creep compliance of solid polymers by nanoindentation. Mech. Time-Depend. Mater. **7**, 189–207 (2003)

Ngan, A.H.W., Wang, H.T., Tang, B., Sze, K.Y.: Correcting power-law viscoelastic effects in elastic modulus measurement using depth-sensing indentation. Int. J. Solids Struct. **42**, 1831–1846 (2005)

Oyen, M.L.: Spherical indentation creep following ramp loading. J. Mater. Res. **20**, 2094–2100 (2005)

Oyen, M.L.: Sensitivity of polymer nanoindentation creep measurements to experimental variables. Acta Mater. **55**, 3633 (2007)

Oyen, M.L., Cook, R.F.J.: Load–displacement behavior during sharp indentation of viscous–elastic–plastic materials. J. Mater. Res. **18**, 139 (2003)

Ramakrishna, S., Huang, Z.M., Kumar, G.V., Batchelor, A.W., Mayer, J.: An Introduction to Biocomposites. Imperial College Press, London (2004)

Shimizu, S., Yanagimoto, T., Sakai, M.: Pyramidal indentation load-depth curve of viscoelastic materials. J. Mater. Res. **14**, 4075–4086 (1999)

Thomas, V., Dean, D.R., Jose, M.V., Mathew, B., Chowdhury, S., Vohra, Y.K.: Nanostructured biocomposite scaffolds based on collagen coelectrospun with nanohydroxyapatite. Biomacromolecules **8**, 631–637 (2007)